

# RSC Advances



This is an *Accepted Manuscript*, which has been through the Royal Society of Chemistry peer review process and has been accepted for publication.

*Accepted Manuscripts* are published online shortly after acceptance, before technical editing, formatting and proof reading. Using this free service, authors can make their results available to the community, in citable form, before we publish the edited article. This *Accepted Manuscript* will be replaced by the edited, formatted and paginated article as soon as this is available.

You can find more information about *Accepted Manuscripts* in the [Information for Authors](#).

Please note that technical editing may introduce minor changes to the text and/or graphics, which may alter content. The journal's standard [Terms & Conditions](#) and the [Ethical guidelines](#) still apply. In no event shall the Royal Society of Chemistry be held responsible for any errors or omissions in this *Accepted Manuscript* or any consequences arising from the use of any information it contains.

Cite this: DOI: 10.1039/c0xx00000x

www.rsc.org/xxxxxx

ARTICLE TYPE

# Mono- and Tri- $\beta$ -Substituted Unsymmetrical Metalloporphyrins: Synthesis, Structural, Spectral and Electrochemical Properties

Kamal Prakash, Ravi Kumar and Muniappan Sankar\*

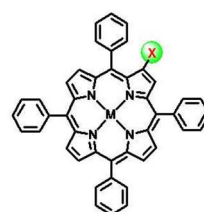
Mono-/tri- $\beta$ -substituted metalloporphyrins, viz. MTPP(X)Y<sub>2</sub> (X = CHO, CH<sub>2</sub>OH, COOH; Y = H, Br, Ph; M = 2H, Co(II), Ni(II), Cu(II), Zn(II)) have been synthesized and characterized. This work examines the influence of  $\beta$ -substitution on structural, electronic spectral and redox properties of MTPP(X) and MTPP(CHO)Y<sub>2</sub>. The redox tunability was achieved by introducing electron donors (CH<sub>2</sub>OH and Ph) and acceptors (CHO, COOH and Br) on MTPP skeleton. Dramatic reduction in HOMO-LUMO gap with considerable increment in  $\Delta\epsilon_{1u}$  was observed as the number of electron withdrawing groups increased. The spectral and electrochemical redox potentials are influenced by the peripheral  $\beta$ -substituents and electronegativity of core metal ion. These porphyrins exhibited tunable electronic spectral and redox properties with modulated frontier orbitals by means of mono- and tri- $\beta$ -substituents which are in direct conjugation with porphyrin  $\pi$ -system. DFT studies of these porphyrins revealed that mono-substituted porphyrins are nearly planar whereas tri-substituted porphyrins have moderate nonplanar conformation.

## Introduction

Metalloporphyrinoids play a vital role in many biological processes.<sup>1</sup> They are ubiquitous in nature and are involved in numerous metabolic processes, such as, oxygen transport and storage, electron transfer, and mono-oxygenation reactions.<sup>1</sup> Metalloporphyrins are also widely studied because of their use in catalytic,<sup>2</sup> photodynamic therapy (PDT),<sup>3</sup> nonlinear optical (NLO)<sup>4</sup> and dye-sensitized solar cell (DSSC)<sup>5</sup> applications. Porphyrin skeleton has an extended  $\pi$ -conjugated system,<sup>6</sup> leading to a wide range of visible light absorption and facile incorporation of various metal ions. The reversibility of the redox chemistry shown by porphyrin i.e. the stability of both their mono- and di-cationic species, makes them particularly attractive for photoionization and photoconductive processes.<sup>7</sup> Such studies are well documented in the mimicking of the photosynthetic reaction centre by photoinduced electron transfer (PET) with use of porphyrin based electron reservoirs.<sup>7</sup> Porphyrins can be designed and tailored for such applications by controlling the substituents attached at the periphery of the macrocycle and also by varying the core metal ion.

The functionalized porphyrins are of considerable importance owing to their use as biomimetic compounds<sup>8</sup> and also for their interesting physicochemical properties.<sup>9</sup> The introduction of substituents at the  $\beta$ -pyrrolic positions has a dramatic influence on the porphyrin  $\pi$ -system<sup>9a,10</sup> rather than their introduction at the *meso*-positions. Due to extensive conjugation of porphyrin  $\pi$ -electrons, the electron withdrawing and donating substituent(s) on the periphery have been shown to affect the basicity of the inner core nitrogens.<sup>11</sup> This, in turn, affects the visible absorption spectra, redox potentials, and axial ligation behaviour of free base and/or their respective metalloporphyrin complexes<sup>11a,12</sup> and they serve as materials or compounds with unusual properties.<sup>13</sup>

Among the synthetic porphyrin analogues, *meso*-tetraphenylporphyrin (H<sub>2</sub>TPP) and its metal complexes (MTPP) are the most widely explored systems because of their ease of synthesis and facile functionalization.  $\beta$ -formyl porphyrin is an important precursor for Horner-Emmons, Wittig, Grignard, McMurry, Schiff base, Knoevenagel and 1,3-dipolar cycloaddition reactions.<sup>14</sup>



$\beta$ -mono-substituted porphyrins



$\beta$ -tri-substituted porphyrins

| X                  | M  | NAME                                     | CODE |
|--------------------|----|--|------|
| CHO                | Zn | H <sub>2</sub> TPP(CHO)                  | 1    |
|                    | Zn | ZnTPP(CHO)                               | 1a   |
|                    | Cu | CuTPP(CHO)                               | 1b   |
|                    | Co | CoTPP(CHO)                               | 1c   |
|                    | Ni | NiTPP(CHO)                               | 1d   |
| CH <sub>2</sub> OH | Zn | H <sub>2</sub> TPP(CH <sub>2</sub> OH)   | 2    |
|                    | Zn | ZnTPP(CH <sub>2</sub> OH)                | 2a   |
|                    | Cu | CuTPP(CH <sub>2</sub> OH)                | 2b   |
|                    | Co | CoTPP(CH <sub>2</sub> OH)                | 2c   |
|                    | Ni | NiTPP(CH <sub>2</sub> OH)                | 2d   |
| COOH               | Zn | H <sub>2</sub> TPP(COOH)                 | 3    |
|                    | Zn | ZnTPP(COOH)                              | 3a   |
|                    | Cu | CuTPP(COOH)                              | 3b   |
|                    | Co | CoTPP(COOH)                              | 3c   |
|                    | Ni | NiTPP(COOH)                              | 3d   |
| Y                  | M  | NAME                                     | CODE |
| Br                 | Zn | H <sub>2</sub> TPP(CHO)Br <sub>2</sub>   | 4    |
|                    | Zn | ZnTPP(CHO)Br <sub>2</sub>                | 4a   |
|                    | Cu | CuTPP(CHO)Br <sub>2</sub>                | 4b   |
|                    | Co | CoTPP(CHO)Br <sub>2</sub>                | 4c   |
|                    | Ni | NiTPP(CHO)Br <sub>2</sub>                | 4d   |
| Ph                 | Zn | H <sub>2</sub> TPP(CHO)(Ph) <sub>2</sub> | 5    |
|                    | Zn | ZnTPP(CHO)(Ph) <sub>2</sub>              | 5a   |
|                    | Cu | CuTPP(CHO)(Ph) <sub>2</sub>              | 5b   |
|                    | Co | CoTPP(CHO)(Ph) <sub>2</sub>              | 5c   |
|                    | Ni | NiTPP(CHO)(Ph) <sub>2</sub>              | 5d   |

Chart 1. Molecular structures of mono/tri- $\beta$ -substituted porphyrins and their metal complexes employed in this study.

MTPP complexes bearing substituent at  $\beta$ -positions or *meso*-positions have been examined by various groups.<sup>15-20</sup> Previous reports have shown that the number of  $\beta$ -substituents and the non-planarity of the macrocycle influence the redox properties of porphyrin  $\pi$ -system.<sup>21,22</sup> The synthesis and electronic properties

of mixed antipodal  $\beta$ -substituted porphyrins have not been much explored<sup>23</sup> possibly due to the lack of synthetic methodologies. This work examines the influence of  $\beta$ -substitution on structural, electronic spectral and electrochemical redox properties of mono- and tri- $\beta$ -substituted *meso*-tetraphenylporphyrins and their metal (Co(II), Ni(II), Cu(II) and Zn(II)) complexes (Chart 1). The substituents such as CHO, COOH, CH<sub>2</sub>OH, Br and Ph at  $\beta$ -position(s) were found to alter the electronic properties of the porphyrin  $\pi$ -system as compared to MTPPs. DFT optimised geometries of **1-5** have also been shown for structural interest. Herein, the consequences of  $\beta$ -substitution have been revealed by various spectroscopic and electrochemical studies of  $\beta$ -formyl metalloporphyrins and their derivatives for the first time.

## Experimental Section

### Materials

2-formyl-*meso*-tetraphenylporphyrin (**1**), 2-hydroxymethyl-*meso*-tetraphenylporphyrin (**2**), 2-carboxy-*meso*-tetraphenylporphyrin (**3**), 2-formyl-12,13-dibromo-*meso*-tetraphenylporphyrin (**4**) and 2-formyl-12,13-diphenyl-*meso*-tetraphenylporphyrin (**5**) were synthesised using modified reported procedures.<sup>24-26</sup> All solvents employed in the present study were of analytical grade and were distilled before use. N-Bromosuccinimide was purchased from HiMedia, India and used after recrystallisation. Copper(II) acetate monohydrate, Zinc(II) acetate dihydrate, Cobalt(II) acetate tetrahydrate and K<sub>2</sub>CO<sub>3</sub> were purchased from HiMedia and Nickel(II) acetate tetrahydrate was purchased from Sigma-Aldrich and used as received. Tetrakis(triphenylphosphine) palladium(0), and phenylboronic acid were obtained from Sigma-Aldrich and used as received.

### Instrumentation and methods

UV-Visible and fluorescence spectra were recorded in CH<sub>2</sub>Cl<sub>2</sub> using Cary 100 spectrophotometer and Hitachi F-4600 spectrofluorometer, respectively. All <sup>1</sup>H NMR measurements were performed using Bruker AVANCE 500 MHz and JEOL 400 MHz spectrometers in CDCl<sub>3</sub>. MALDI-TOF mass spectra were measured using a Bruker UltrafleXtreme-TN MALDI-TOF/TOF spectrometer using HABA (4'-hydroxyazobenzene-2-carboxylic acid) as a matrix. Electrochemical measurements were carried out using CHI-620E instrument. A three electrode system was used which consisted of a Pt Working electrode, Ag/AgCl reference and a Pt-wire counter electrode. The concentrations of all porphyrins employed were ~1 mM. All measurements were performed in triple distilled CH<sub>2</sub>Cl<sub>2</sub> which was purged with Ar gas, using 0.1 M TBAPF<sub>6</sub> as the supporting electrolyte.

### Synthesis of Co(II) and Ni(II) complexes (**1c-5c** and **1d-5d**) of H<sub>2</sub>TPP(X)Y<sub>2</sub> (X = CHO, COOH, CH<sub>2</sub>OH; Y = H, Br, Ph):

H<sub>2</sub>TPP(X)Y<sub>2</sub> (100 mg) was taken in 500 mL RB flask containing 150 mL of CHCl<sub>3</sub>. To this, 10 equiv. of M(OAc)<sub>2</sub> hydrate (M = Cu(II), Zn(II), Co(II)) in 20 mL of methanol was added and refluxed for 20 minutes and the reaction mixture was cooled to room temperature, washed with water and dried over anhydrous sodium sulphate. The crude product was purified by column chromatography on silica gel column using CHCl<sub>3</sub> as eluent. Yield was found to be 53-92%. In case of Ni metallation, H<sub>2</sub>TPP(X)Y<sub>2</sub> (100 mg) was dissolved in 50 mL DMF and

refluxed for 3 hours and cooled to RT. To this, 200 mL of distilled water was added to precipitate the porphyrin, filtered and purified on silica column using CHCl<sub>3</sub> as eluent. Yield was found to be 56-82%.

**1c-5c** were prepared from their corresponding H<sub>2</sub>TPP(X)Y<sub>2</sub> with the yield of 53 - 92%. **1c**: 92% yield. UV-Vis. (CH<sub>2</sub>Cl<sub>2</sub>,  $\lambda_{\max}$  in nm): 422 (5.33), 539 (3.51), 577 (3.38). MALDI-TOF-MS: *m/z* 700.24 for [M+H]<sup>+</sup> (calcd. 700.17). Anal. Calcd. for C<sub>45</sub>H<sub>28</sub>N<sub>4</sub>OCo: C, 77.25; H, 4.03; N, 8.01%. Found: C, 77.13; H, 3.91; N, 8.27%. **2c**: 70% yield. UV-Vis. (CH<sub>2</sub>Cl<sub>2</sub>,  $\lambda_{\max}$  in nm): 409 (5.38), 528 (4.14). MALDI-TOF-MS: *m/z* 701.35 for [M]<sup>+</sup> (calcd. 701.18). Anal. Calcd. for C<sub>45</sub>H<sub>30</sub>N<sub>4</sub>OCo: C, 77.03; H, 4.31; N, 7.98%. Found: C, 77.18; H, 4.21; N, 7.75%. **3c**: 53% yield. UV-Vis. (CH<sub>2</sub>Cl<sub>2</sub>,  $\lambda_{\max}$  in nm): 416 (5.23), 535 (4.04). MALDI-TOF-MS: *m/z* 715.47 for [M]<sup>+</sup> (calcd. 715.15). Anal. Calcd. for C<sub>45</sub>H<sub>28</sub>N<sub>4</sub>O<sub>2</sub>Co: C, 75.52; H, 3.94; N, 7.83%. Found: C, 75.32; H, 3.78; N, 7.73%. **4c**: 70% yield. UV-Vis. (CH<sub>2</sub>Cl<sub>2</sub>,  $\lambda_{\max}$  in nm): 428 (5.18), 549 (3.98), 589 (4.00). MALDI-TOF-MS: *m/z* 854.73 for [M]<sup>+</sup> (calcd. 854.98). Anal. Calcd. for C<sub>45</sub>H<sub>26</sub>Br<sub>2</sub>N<sub>4</sub>OCo: C, 63.03; H, 3.06; N, 6.53%. Found: C, 63.11; H, 3.00; N, 6.60%. **5c**: 60% yield. UV-Vis. (CH<sub>2</sub>Cl<sub>2</sub>,  $\lambda_{\max}$  in nm): 429 (4.96), 550 (3.81), 587 (3.80). MALDI-TOF-MS: *m/z* 858.28 for [M+Li]<sup>+</sup> (calcd. 858.24). Anal. Calcd. for C<sub>57</sub>H<sub>36</sub>N<sub>4</sub>OCo: C, 80.37; H, 4.26; N, 6.58%. Found: C, 80.25; H, 4.32; N, 6.41%.

**1d-5d** were synthesised from their corresponding H<sub>2</sub>TPP(X)Y<sub>2</sub> with the yield of 56 - 82%.

**1d**: 80% yield. UV-Vis. (CH<sub>2</sub>Cl<sub>2</sub>,  $\lambda_{\max}$  in nm): 426 (5.22), 540 (4.06), 580 (3.94). <sup>1</sup>H NMR (CDCl<sub>3</sub>, 400MHz):  $\delta$  (ppm) 9.31 (s, 1H, CHO), 9.16 (s, 1H,  $\beta$ -Pyrrole-H), 8.67-8.74 (m, 6H,  $\beta$ -Pyrrole-H), 7.95-8.02 (m, 8H, *o*-PhH), 7.66-7.72 (m, 12H, *m*- and *p*-PhH). MALDI-TOF-MS: *m/z* 700.02 for [M+H]<sup>+</sup> (calcd. 700.43). Anal. Calcd. for C<sub>45</sub>H<sub>28</sub>N<sub>4</sub>ONi: C, 77.28; H, 4.04; N, 8.01%. Found: C, 77.09; H, 4.08; N, 8.08%.

**2d**: 82% yield. UV-Vis. (CH<sub>2</sub>Cl<sub>2</sub>,  $\lambda_{\max}$  in nm): 414 (5.31), 529 (4.16). <sup>1</sup>H NMR (CDCl<sub>3</sub>, 400 MHz):  $\delta$  (ppm) 8.80 (s, 1H,  $\beta$ -Pyrrole-H), 8.66-8.72 (m, 6H,  $\beta$ -Pyrrole-H), 7.96-7.99 (m, 6H, *o*-PhH), 7.88 (d, *J* = 6.8 Hz, 2H, *o*-PhH), 7.65-7.67 (m, 12H, *m*- and *p*-PhH), 4.75 (d, *J* = 5.6 Hz, 2H, -CH<sub>2</sub>), 1.83 (bt, 1H, -OH). MALDI-TOF-MS: *m/z* 701.25 for [M+H]<sup>+</sup> (calcd. 701.19). Anal. Calcd. for C<sub>45</sub>H<sub>30</sub>N<sub>4</sub>ONi: C, 77.05; H, 4.31; N, 7.99%. Found: C, 76.93; H, 4.09; N, 7.89%.

**3d**: 61% yield. UV-Vis. (CH<sub>2</sub>Cl<sub>2</sub>,  $\lambda_{\max}$  in nm): 422 (5.21), 535 (4.05), 561(sh). <sup>1</sup>H NMR (CDCl<sub>3</sub>, 400MHz):  $\delta$  (ppm) 9.02 (s, 1H,  $\beta$ -Pyrrole-H), 8.65-8.72 (m, 6H,  $\beta$ -Pyrrole-H), 7.92-8.00 (m, 8H, *o*-PhH), 7.65-7.72 (m, 12H, *m*- and *p*-PhH). MALDI-TOF-MS: *m/z* 715.00 for [M+H]<sup>+</sup> (calcd. 715.16). Anal. Calcd. for C<sub>45</sub>H<sub>28</sub>N<sub>4</sub>O<sub>2</sub>Ni: C, 75.55; H, 3.94; N, 7.83%. Found: C, 75.38; H, 3.78; N, 7.71%.

**4d**: 56% yield. UV-Vis. (CH<sub>2</sub>Cl<sub>2</sub>,  $\lambda_{\max}$  in nm): 430(5.27), 550(4.03), 594(4.04). <sup>1</sup>H NMR (CDCl<sub>3</sub>, 400MHz):  $\delta$  (ppm) 9.22 (s, 1H, -CHO), 9.13 (s, 1H,  $\beta$ -Pyrrole-H), 8.66 (d, *J* = 5.6 Hz, 1H,  $\beta$ -Pyrrole-H), 8.61 (ABq, *J* = 5.2 Hz, 3H,  $\beta$ -Pyrrole-H), 7.99 (d, *J* = 6.8Hz, 2H, *o*-PhH), 7.93 (d, *J* = 6Hz, 2H, *o*-PhH) 7.82-7.84 (m, 4H, *o*-PhH), 7.61-7.74 (m, 12H, *m*- and *p*-PhH). MALDI-TOF-MS: *m/z* 856.07 for [M]<sup>+</sup> (calcd. 855.98). Anal. Calcd. for C<sub>45</sub>H<sub>26</sub>Br<sub>2</sub>N<sub>4</sub>ONi: C, 63.05; H, 3.06; N, 6.54%. Found: C, 63.16; H, 3.23; N, 6.46%.

**5d:** 74% yield. UV-Vis. ( $\text{CH}_2\text{Cl}_2$ ,  $\lambda_{\text{max}}$  in nm): 432(5.32), 556(4.06), 596(3.98).  $^1\text{H}$  NMR ( $\text{CDCl}_3$ , 400MHz):  $\delta$  (ppm) 9.24(s, 1H, CHO), 9.17(s, 1H,  $\beta$ -Pyrrole-H), 8.55(dd,  $J = 10$  Hz, 5.2 Hz, 2H,  $\beta$ -Pyrrole-H), 8.29(dd,  $J = 10.4$  Hz, 4.8 Hz, 2H,  $\beta$ -pyrrole-H), 7.93-8.00(m, 4H, *meso*-PhH), 7.64-7.70(m, 6H, *meso*-PhH), 7.43(d,  $J = 8$  Hz, 4H, *meso*-PhH), 7.15-7.17(m, 2H, *meso*-PhH), 7.04-7.08(m, 4H, *meso*-PhH), 6.81-6.88(m, 10H,  $\beta$ -Pyrrole-PhH). MALDI-TOF-MS:  $m/z$  853.28 for  $[\text{M}]^+$  (calcd. 853.22). Anal. Calcd. for  $\text{C}_{57}\text{H}_{36}\text{N}_4\text{O}$ : C, 80.39; H, 4.26; N, 6.58%. Found: C, 80.17; H, 4.22; N, 6.43%.

## Results and Discussion

### Synthesis and Characterization

We have synthesized a series of  $\beta$ -substituted porphyrins (**2-5**) starting from **1** and their metal complexes as shown in scheme S1 in the electronic supplementary information (ESI). **1** was prepared using Vilsmeier-Haack reaction in good yields (70-90%).<sup>24</sup> The presence of a formyl group localizes the double bond at an antipodal  $\beta$ -pyrrolic position<sup>25</sup> which can be easily brominated. **1** was selectively dibrominated using 2.5 equivalent of NBS at 50 - 60 °C in which product formation occurs within 24 hours with 60% yield in contrast to time consuming reported procedure.<sup>25a</sup>  $\text{H}_2\text{TPP}(\text{CHO})\text{Ph}_2$  (**5**) was prepared from **4** using a modified Suzuki cross coupling reaction with 60% yield. **1** was reduced using  $\text{NaBH}_4$  in dry ethanol to afford **2** in 90% yield and also oxidized using hydroxylamine hydrochloride and phthalic anhydride mixture<sup>26</sup> to get **3** in 70% yield. Metal (Zn(II), Cu(II), Co(II) and Ni(II)) complexes of free base porphyrins (**1-5**) were also synthesized in moderate to good yields (50-95%) using conventional methods.<sup>23c</sup> These porphyrins were characterized by UV-Vis, fluorescence,  $^1\text{H}$  NMR spectroscopic techniques and mass spectrometry analysis. The antipodal regioselective  $\beta$ -dibromination of  $\text{H}_2\text{TPP}(\text{CH}_2\text{OH})$  (**2**) and  $\text{H}_2\text{TPP}(\text{COOH})$  (**3**) using NBS was unsuccessful and ended with mixture of products. We also attempted tri-, tetra-, penta- and hexa-bromination of  $\text{H}_2\text{TPP}(\text{X})$  ( $\text{X} = \text{CHO}, \text{COOH}, \text{CH}_2\text{OH}$ ) by using varying amounts of NBS or liquid  $\text{Br}_2$  in  $\text{CHCl}_3$  which resulted only in the degradation of porphyrins.

### DFT Studies

The ground state geometries of mono- and tri-substituted free base porphyrins (**1-5**) were optimized in the gas phase by DFT calculations using the B3LYP functional and 6-311g(d,p) basis set.<sup>27</sup> Figures 1 and S1 in ESI represent the fully optimized geometries of these porphyrins (top and side views) as well as the deviation of core atoms from the porphyrin mean plane. Selected averages bond length and bond angles of mono and tri-substituted are listed in the Table S1 in ESI. The enhancement in non-planarity of porphyrins is observed when pyrrole ring bends to adjust the repulsive interaction between substituent present at the  $\beta$ -pyrrole position. The bending of pyrrole of porphyrin ring has three consequences; (a)  $\text{C}_\beta\text{-C}_\beta$  bond length increases, (b)  $\text{C}_\beta\text{-C}_\alpha\text{-C}_m$  bond angles increases and (c)  $\text{N-C}_\alpha\text{-C}_m$  bond angle decreases which leads to non-planarity of porphyrin ring. Mono-substituted porphyrin (**1-3**) exhibited slight distortion from the mean plane of porphyrin. **2** has nearly planar structure whereas **1** and **3** exhibited slightly non-planar conformation from the mean plane. Tri-substituted porphyrins (**4** and **5**) exhibited moderate non-

planarity from the mean plane as compared to the **1-3** porphyrins. The non-planarity of tri-substituted porphyrins (**4** and **5**) is shown from the increment in  $\text{C}_\beta\text{-C}_\beta$  bond length as well as in the  $\text{C}_\beta\text{-C}_\alpha\text{-C}_m$  bond angles along with the decrement of  $\text{N-C}_\alpha\text{-C}_m$  bond angle. Tri-substituted porphyrins (**4** and **5**) showed 1-2° more change in these angles as compared to mono-substituted porphyrin (**1-3**). These results of tri-substituted porphyrins are comparable to di- and tri-substituted porphyrins reported in literature.<sup>25b,28</sup>  $\text{H}_2\text{TPPBr}_2$  has quasi-planar structure whereas  $\text{ZnTPP}(\text{Ph})_2$  and  $\text{H}_2\text{TPP}(\text{Ph})_4$ <sup>29</sup> are nearly planar structure. But  $\text{H}_2\text{TPP}(\text{NO}_2)(\text{Ph})_2$  and  $\text{H}_2\text{TPP}(\text{CHO})(\text{Ph})_2$  exhibited moderate non-planarity. The moderate non-planarity of  $\text{H}_2\text{TPP}(\text{CHO})(\text{Ph})_2$  as reflected in our DFT studies is in agreement with its crystal structure.<sup>25a</sup>

Fig. 1 shows the side view and top view of  $\text{H}_2\text{TPP}(\text{CHO})\text{Br}_2$  and  $\text{H}_2\text{TPP}(\text{CHO})(\text{Ph})_2$ . The deviation of porphyrin core carbon atoms from the mean plane is shown in figures 1e and 1f which reflects the moderate non-planarity of compound **4** and **5**. The substituents (formyl, carboxy and hydroxyl group) present in mono-substituted porphyrin (**1-3**) exhibited lower  $\Delta z$  ( $\pm 0.118$ - $0.346$  Å) from the porphyrin mean plane (i.e. almost planar structure) as compared to the displacement of  $\Delta z$  ( $\pm 0.482$ - $0.697$  Å) of substituent (formyl, bromine and phenyl group) present in tri-substituted porphyrin (**4** and **5**).

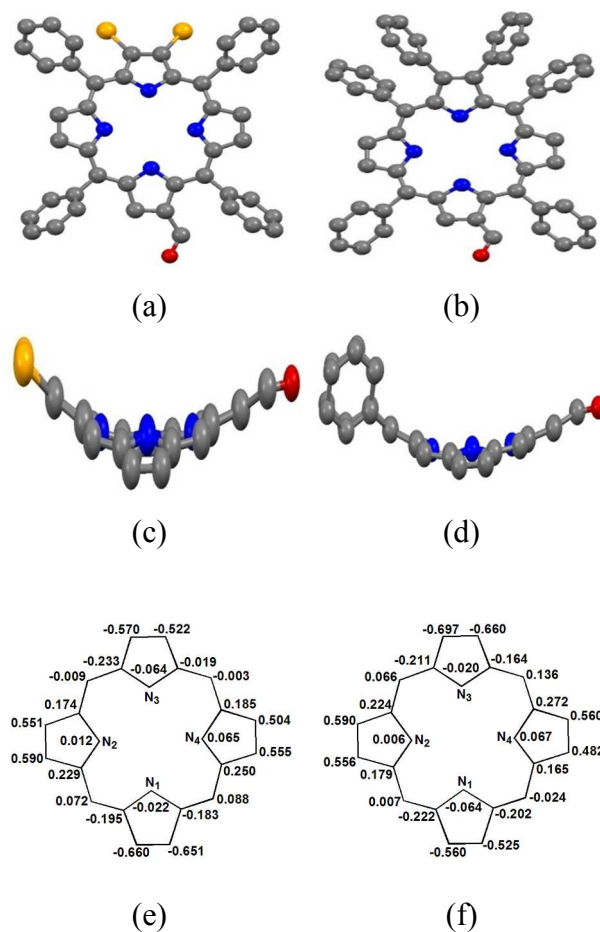


**Fig.1.** B3LYP/6-311G(d,p) optimised geometries showing top (a and b) as well as side view (c and d) of **4** and **5** respectively. In side view, the *meso*-phenyl group are not shown for clarity. e and f is showing the displacement of porphyrin core atoms (in Angstrom) from the mean plane of **4** and **5** respectively. Color codes for atoms: C, black; O, red; N, blue; Br, brown.

Same trend has been followed by  $\beta$ -pyrrole carbon atoms as we move from mono- to tri-substituted porphyrin which is similar as we move from  $H_2TPP(NO_2)(X)_2$  to  $H_2TPP(NO_2)(X)_6$ .<sup>28b</sup> These observations confirm that the extent of steric crowding at the  $\beta$ -pyrrole position and bumping of the core imino protons are counterbalanced by the conformation flexibility of the porphyrin ring which results in the moderate non-planarity of tri-substituted porphyrins as compared to mono-substituted porphyrins. The mean plane displacement of the  $\beta$ -pyrrole carbons ( $\Delta C_\beta$ ) from the mean plane follows the order:  $H_2TPP(CH_2OH)(2) < H_2TPP(CHO)(1) < H_2TPP(COOH)(3) < H_2TPP(CHO)Br_2(4) < H_2TPP(CHO)(Ph)_2(5)$  indicating the varying degree of non-planarity in these mixed substituted porphyrins.

### 15 Electronic Spectral and NMR Studies

The electronic spectra of porphyrins are influenced by the presence of peripheral  $\beta$ -substituents and core metal ions. The electronic absorption spectra of  $H_2TPP(X)Y_2$  exhibited a Soret (B band) and four Q bands which are similar to that of  $H_2TPP$ . Table 1 lists the optical absorption spectral data of  $MTPP(X)Y_2$  ( $M = 2H$  and  $Zn(II)$ ) in  $CH_2Cl_2$  at 298 K. The optical absorption spectra of **1-3** are shown in Figure 2.  $H_2TPP(X)Y_2$  ( $X = CHO, COOH; Y = H, Br, Ph$ ) exhibited red-shifts in B band ( $\Delta\lambda_{max} = 5 - 19$  nm) and  $Q_x(0,0)$  band ( $\Delta\lambda_{max} = 7 - 32$  nm) relative to **2** (Figures S2-S7 in ESI). This is possibly due to the inductive and/or conjugative interaction of the substituents with porphyrin  $\pi$ -system.  $H_2TPPBr_2$ ,  $ZnTPP(CHO)$ ,  $H_2TPP(CHO)Ph_2$  were shown quasi-planar crystal structures as evidenced from the lower mean plane deviation of 24-atom porphyrin core ( $\Delta 24 = 0.08 - 0.17$  Å).<sup>25</sup>

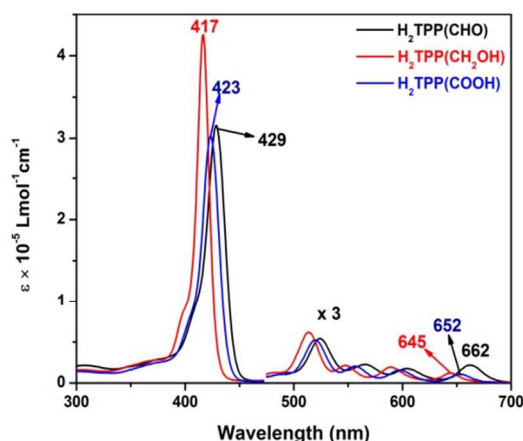


Figure 2. Optical absorption spectra of **1-3** ( $H_2TPP(X)$ ) in  $CH_2Cl_2$  at 298 K.

Notably, **2** exhibited blue-shift in B ( $\Delta\lambda_{max} = 12$  nm) and  $Q_x(0,0)$  bands ( $\Delta\lambda_{max} = 17$  nm) relative to **1** which can be attributed to the influence of electron donating nature of hydroxymethyl group as compared to electron withdrawing CHO substituent. **1** and **3-5** exhibited broadened absorption spectra (FWHM = 21-30 nm) as compared to **2** (FWHM = 15 nm) which is possibly due to intramolecular charge transfer. **5** also showed red-shift in B (7 nm) and  $Q_x(0,0)$  (15 nm) bands as compared to **1** is possibly due to conjugative interaction as well as nearly planar structure of the porphyrin macrocycle with extensive conjugation.<sup>25a</sup>

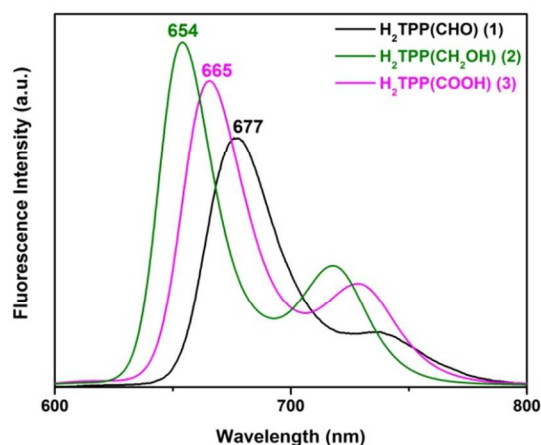


Figure 3. Fluorescence spectra of **1-3** ( $H_2TPP(X)$ ) in  $CH_2Cl_2$  at 298 K.

Notably, the red shift in B and  $Q_x(0,0)$  bands follow the order:  $H_2TPP(CH_2OH)$  (**2**)  $\approx H_2TPP < H_2TPP(COOH)$  (**3**)  $< H_2TPP(CHO)$  (**1**)  $< H_2TPP(CHO)Br_2$  (**4**)  $\approx H_2TPP(CHO)Ph_2$  (**5**). The observed red shift of B and  $Q_x(0,0)$  bands is in accordance with increment in the number of electron withdrawing substituents ( $H_2TPP < H_2TPP(X) < H_2TPP(X)Y_2$ ). These results clearly suggest that by means of mixed substitution one can achieve tunable optical absorption spectral features with considerable red-shift. In case of metal complexes of **1** and **3-5**, one B and one/two Q bands were observed with considerable red-shift in electronic spectral features relative to **2** and  $MTPPs$  as seen in free base porphyrins (tables 1 and S2 in ESI).

Table 1. UV-Vis absorption spectral data<sup>a</sup> of mixed  $\beta$ -substituted free base porphyrins and their  $Zn(II)$  Complexes in  $CH_2Cl_2$  at 298 K.

| Por. | B band, $\lambda_{max}$ , nm | Q bands, $\lambda_{max}$ , nm              | Emission, $\lambda_{ems}$ , nm | Quantum Yield, $\phi_f$ |
|------|------------------------------|--|--------------------------------|-------------------------|
| 1    | 429(5.49)                    | 524(4.25), 566(3.88), 605(3.75), 662(3.85) | 677, 735(sh)                   | 0.1420                  |
| 2    | 417(5.62)                    | 513(4.31), 548(3.84), 589(3.80), 645(3.60) | 654, 716(sh)                   | 0.1132                  |
| 3    | 423(5.48)                    | 520(4.24), 556(3.83), 597(3.71), 652(3.54) | 665, 728(sh)                   | 0.0913                  |
| 4    | 434(5.40)                    | 531(4.18), 565(3.60), 615(3.47), 675(3.89) | 707                            | 0.0025                  |
| 5    | 436(5.77)                    | 531(4.55), 572(4.61), 610(4.47), 677(4.11) | 712                            | 0.0560                  |
| 1a   | 430(5.56)                    | 558(4.20), 601(4.04)                       | 621                            | 0.0209                  |
| 2a   | 418(5.67)                    | 547(4.29), 583(sh)                         | 600(sh), 646                   | 0.0266                  |
| 3a   | 425(5.50)                    | 553(4.22), 592(3.68)                       | 608, 656                       | 0.0279                  |
| 4a   | 434(5.47)                    | 562(4.08), 606(4.05)                       | 634                            | 0.0009                  |
| 5a   | 436(5.37)                    | 563(4.04), 606(3.93)                       | 647                            | 0.0091                  |

<sup>a</sup>The values in parentheses refer to  $\log \epsilon$  values,  $\epsilon$  in  $dm^3/mol/cm$ ; Por = Porphyrin; sh = shoulder; error in quantum yield values  $\pm 1-2\%$ .

The molar absorption coefficients of  $MTPP(X)Y_2$  are not significantly different from that of  $MTPPs$ . The extended conjugation and inductive interaction of  $\beta$ -substituent(s) with the

porphyrin  $\pi$ -system<sup>30</sup> and moderate nonplanarity of the macrocycle are indicative of enhanced red-shift of the absorption spectral features of these metalloporphyrins.

The synthesized free base and Zn(II) complexes of MTPP(X)Y<sub>2</sub> were characterized by fluorescence spectroscopy to elucidate the role of mono- and tri- $\beta$ -substitution. The representative emission spectra of **1-3** in CH<sub>2</sub>Cl<sub>2</sub> are shown in Figure 3. Table 1 lists the fluorescence spectral data and quantum yields of MTPP(X)Y<sub>2</sub> in CH<sub>2</sub>Cl<sub>2</sub> at 298 K. **1** and **3-5** exhibited red-shifted emission ( $\Delta\lambda_{em}$  = 11 - 53 nm) than that of **2** in CH<sub>2</sub>Cl<sub>2</sub> (Table S3 in the ESI).

The free-base porphyrins exhibited an interesting trend in the red-shift of their corresponding emission bands and aligns in the following order: H<sub>2</sub>TPP(CH<sub>2</sub>OH) (**2**)  $\approx$  H<sub>2</sub>TPP < H<sub>2</sub>TPP(COOH) (**3**) < H<sub>2</sub>TPP(CHO) (**1**) < H<sub>2</sub>TPP(CHO)Ph<sub>2</sub> (**5**). The increasing order of red-shift and the decrement in fluorescence quantum yields is in good agreement with the increment in the number of electron withdrawing groups and conformational features of these porphyrins (Figures S8-S14 in ESI). The same trend was also observed for Zn(II) complexes as expected. Notably, H<sub>2</sub>TPP(CHO)Ph<sub>2</sub> showed a reduced emission intensity possibly due to intramolecular charge transfer which reduces the singlet excited state lifetime in comparison with **1** and **2**. Further, the lower emission intensity of **4** is ascribed to the combination of nonplanarity and heavy atom effect of bromo groups that are in direct conjugation with the porphyrin  $\pi$ -system.

The main feature of protons resonance of porphyrins is  $\beta$ -pyrrole, *meso*-phenyl and imino protons. Mono-/tri- $\beta$ -substituted porphyrins having different substituent(s) on  $\beta$ -pyrrole positions also affect the proton resonance of these porphyrins (Figures S15-S24 in ESI). The proton resonance of MTPP(CHO)Y<sub>2</sub> (Y = H, Br, Ph) have the characteristic signal of formyl group and adjacent  $\beta$ -pyrrole-H which appear in the range of 9.13 - 9.50 ppm. The signals of formyl proton for **4** and **5** are upfield shifted by  $\sim$  0.1 ppm relative to **1**. The  $\beta$ -pyrrole protons of **5** shows two doublets at 8.55 and 8.74, respectively and are upfielded by 0.11 - 0.30 ppm with respect to **4** which shows one singlet for  $\beta$ -pyrrole-H at 8.85 ppm. Further, the  $\beta$ -pyrrole protons of **4** are slightly downfield shifted than **1**. There is no much difference between the signals for *meso*-aryl protons of H<sub>2</sub>TPP(CHO) and H<sub>2</sub>TPP(CHO)Br<sub>2</sub> which appears in the range of 7.73 - 8.25 ppm whereas H<sub>2</sub>TPP(CHO)Ph<sub>2</sub> exhibit the upfielded signals of *meso*-phenyl protons due to electron donating nature of Ph groups. The  $\beta$ -pyrrole phenyl protons of **5** appear in the range of 6.84 - 6.89 ppm. Interestingly, imino protons resonance of **1** shows singlet at -2.56 ppm which is downfield shifted as compared to **4** (-2.71 ppm) and upfield shifted to **5** (-2.25 ppm). There was no signal appeared for  $\beta$ -carboxy proton of MTPP(COOH) in CDCl<sub>3</sub> whereas MTPP(CH<sub>2</sub>OH) have characteristic feature of proton resonance due to CH<sub>2</sub>O and OH protons which are exhibiting broad doublets (4.75 - 4.91 ppm) and triplet (1.83 - 1.97 ppm), respectively. The  $\beta$ -pyrrolic proton resonances of **3** exhibit downfield shift (8.80 - 8.84 ppm) by 0.1 ppm with respect to  $\beta$ -pyrrole-H of **2** (8.77 - 8.94 ppm). The proton resonances of *meso*-aryl protons in **3** are not much different than those of **1** and **2**. The imino protons of **3** and **2** show proton resonances at -2.67 and

-2.77 ppm, respectively which are upfielded as compared to **1** (-2.53 ppm). The <sup>1</sup>H NMR spectra of metal complexes of **1-5** are devoid of imino-protons revealing that metal ion got inserted into the porphyrin ring. The  $\beta$ -pyrrole and *meso*-phenyl protons resonance of Ni(II) complexes are marginally upfield shifted whereas Zn(II) complexes are marginally downfield shifted as compared to their corresponding free-base derivatives. The integrated intensities of the proton resonances of these mono- and tri- $\beta$ -substituted porphyrins are in consistent with the proposed structures.

### Electrochemical Studies

The electrochemical studies were performed on mixed substituted porphyrins (MTPP(X)Y<sub>2</sub>) to investigate the effect of the  $\beta$ -substitution on the porphyrin  $\pi$ -system.

The electrochemical redox data of MTPP(X)Y<sub>2</sub> are summarized in table 2. Figure 4 presents the cyclic voltammograms (CVs) of CuTPP(X)Y<sub>2</sub> bearing different  $\beta$ -pyrrole substituent(s) in CH<sub>2</sub>Cl<sub>2</sub> containing 0.1 M TBAPF<sub>6</sub> at 298 K. These porphyrins exhibited two successive ring centred one-electron oxidation and two one-electron reduction potentials. In case of Co(II) complexes, the first oxidation and reduction are found to originate from metal centre. For comparison, MTPPs were also examined under similar conditions and the data is presented in table 2. The observed redox potentials of MTPP(X)Y<sub>2</sub> were chosen to delineate the effect of  $\beta$ -substitution on the redox properties of the porphyrin macrocycle. The CVs of MTPP(X)Y<sub>2</sub> other than Cu(II) complexes were presented in ESI (Figures S25 -S26). The data analysis of MTPP(X)Y<sub>2</sub> revealed the following facts: (1) The first ring oxidation potentials of MTPP(X)Y<sub>2</sub> range from 0.84 to 1.18 V whereas first ring reduction potentials show a wide range from -0.89 to -1.43V. (2) By appending electron donor substituent such as hydroxymethyl, we could observe a marginal cathodic shift in their first ring oxidation (0.01 - 0.04 V) and reduction (0.01 - 0.13 V) potentials in comparison to MTPP whereas an opposite trend was observed for COOH substituent i.e. MTPP(COOH). (3) While appending electron acceptor substituents such as CHO, Br, COOH groups, a dramatic anodic shift in their reduction (0.15 - 0.39 V) and oxidation (0.1 - 0.22 V) potentials were observed as compared to MTPPs indicating extensive stabilization of LUMO. (4) MTPP(CHO) exhibited an anodic shift in their reduction (0.18 - 0.24 V) and oxidation potentials (0.05 - 0.1 V) with respect to MTPP due to electron withdrawing nature of CHO substituent. MTPP(CHO)Br<sub>2</sub> showed further anodic shift in their oxidation (0.05 - 0.22 V) and reduction potentials (0.04 - 0.17 V) as compared to MTPP(CHO). (6) On the other hand, MTPP(CHO)Ph<sub>2</sub> exhibited a cathodic shift in their oxidation potentials (0.02 - 0.13 V) whereas reduction potentials are almost unaltered indicating the electron donating nature of phenyl substituents. (7) Further, MTPP(CHO)Br<sub>2</sub> exhibited anodic shift in their first oxidation potentials (0.1 - 0.22 V) and in their first reduction potentials (0.19 - 0.39 V) with respect to MTPP(CH<sub>2</sub>OH).

**Table 2.** Redox data (vs Ag/AgCl) of MTPP(X)Y<sub>2</sub> in CH<sub>2</sub>Cl<sub>2</sub> containing TBAPF<sub>6</sub> as supporting electrolyte at 298 K.

| Por.               | Oxidation (V)     |                   | $\Delta E_{1/2}^b$ (V) | Reduction (V)      |                    | Metal Centred     |                    |
|--------------------|-------------------|-------------------|------------------------|--------------------|--------------------|-------------------|--------------------|
|                    | I                 | II                |                        | I                  | II                 | Ox.               | Red.               |
| H <sub>2</sub> TPP | 1.00              | 1.34              | 2.23                   | -1.23              | -1.54              |                   |                    |
| <b>1</b>           | 1.05              | 1.26              | 2.04                   | -0.99              | -1.25              |                   |                    |
| <b>2</b>           | 0.97 <sup>i</sup> | 1.50              | 2.19                   | -1.22              | -1.55              |                   |                    |
| <b>3</b>           | 1.00              | 1.50 <sup>a</sup> | 2.04                   | -1.04 <sup>i</sup> | -1.28              |                   |                    |
| <b>4</b>           | 1.11              | 1.22              | 2.00                   | -0.89              | -                  |                   |                    |
| <b>5</b>           | 1.00              | 1.11              | 2.00                   | -1.00              | -1.17              |                   |                    |
| ZnTPP              | 0.84              | 1.15              | 2.20                   | -1.36              | -1.77              |                   |                    |
| <b>1a</b>          | 0.88              | 1.17              | 2.01                   | -1.13              | -1.46              |                   |                    |
| <b>2a</b>          | 0.84              | 1.10              | 2.24                   | -1.40 <sup>i</sup> | -1.73 <sup>i</sup> |                   |                    |
| <b>3a</b>          | 0.84              | 1.14              | 2.12                   | -1.28              | -                  |                   |                    |
| <b>4a</b>          | 0.94              | 1.19              | 2.11                   | -1.17 <sup>a</sup> | -1.41 <sup>a</sup> |                   |                    |
| <b>5a</b>          | 0.86              | 1.07              | 1.97                   | -1.11 <sup>i</sup> | -1.31              |                   |                    |
| CuTPP              | 0.97              | 1.35              | 2.27                   | -1.30              | -1.70              |                   |                    |
| <b>1b</b>          | 1.06              | 1.42              | 2.16                   | -1.10 <sup>i</sup> | -1.42              |                   |                    |
| <b>2b</b>          | 0.96              | 1.31              | 2.39                   | -1.43 <sup>i</sup> | -1.65 <sup>i</sup> |                   |                    |
| <b>3b</b>          | 1.00              | 1.35              | 2.11                   | -1.11 <sup>i</sup> | -1.29 <sup>i</sup> |                   |                    |
| <b>4b</b>          | 1.07              | 1.46              | 2.04                   | -0.97              | -1.21              |                   |                    |
| <b>5b</b>          | 0.93              | 1.33              | 2.04                   | -1.11              | -1.40              |                   |                    |
| CoTPP              | 1.06              | 1.32              | 2.44                   | -1.38              | -                  | 0.85              | -0.86              |
| <b>1c</b>          | 1.14              | 1.36              | 2.30                   | -1.16              | -1.47 <sup>a</sup> | 0.89              | -0.76              |
| <b>2c</b>          | 1.11 <sup>a</sup> | 1.31 <sup>a</sup> | 2.45                   | -1.34 <sup>a</sup> | -1.92 <sup>a</sup> | 0.88 <sup>a</sup> | -0.85 <sup>a</sup> |
| <b>3c</b>          | 1.18              | 1.34 <sup>i</sup> | 2.23                   | -1.05 <sup>i</sup> | -                  | 0.76              | -0.88 <sup>i</sup> |
| <b>4c</b>          | 1.17              | 1.36              | 2.16                   | -0.99 <sup>a</sup> | -1.43 <sup>a</sup> | 0.90              | -0.60              |
| <b>5c</b>          | 1.07              | 1.25              | 2.20                   | -1.13 <sup>a</sup> | -1.49 <sup>a</sup> | 0.88              | -0.73              |
| NiTPP              | 1.02              | 1.32              | 2.30                   | -1.28              | -1.72              |                   |                    |
| <b>1d</b>          | 1.10              | 1.31              | 2.20                   | -1.10              | 1.44               |                   |                    |
| <b>2d</b>          | 1.01              | 1.30              | 2.41                   | -1.40 <sup>i</sup> | -1.65 <sup>i</sup> |                   |                    |
| <b>3d</b>          | 1.08              | 1.28              | 2.33                   | -1.25 <sup>i</sup> | -                  |                   |                    |
| <b>4d</b>          | 1.24              | -                 | 2.20                   | -0.96              | -1.20              |                   |                    |
| <b>5d</b>          | 1.07              | 1.30              | 2.17                   | -1.10              | -1.40              |                   |                    |

Scan rate = 0.1 V/s. <sup>a</sup>Data taken from DPV. <sup>i</sup>Irreversible oxidation or reduction. <sup>b</sup> $\Delta E_{1/2} = E_{1/2}^{\text{oxd.}} - E_{1/2}^{\text{red.}}$ . Pt working and Pt wire counter electrodes were used.

So the general trend in their first redox potentials of MTPP(X)Y<sub>2</sub> is shown below: MTPP(CHO)Br<sub>2</sub> > MTPP(CHO) > MTPP(CHO)(Ph)<sub>2</sub> ≥ MTPP(COOH) > MTPP ≥ MTPPP(CH<sub>2</sub>OH).

In general, the oxidation potentials are largely influenced by the electronic nature of the substituent and non-planarity of the macrocycle while reduction potential are independent of structural changes.<sup>21,22,31</sup> The unusual shift in redox potentials of MTPP(X)Y<sub>2</sub> can be ascribed to the electronic nature of substituent(s) present at  $\beta$ -pyrrole position of porphyrin macrocycle rather than non-planarity. Interestingly, the anodic shift in ring reduction potentials of MTPP(X)Y<sub>2</sub> exhibited more pronounced anodic shift in reduction (0.19 - 0.39 V) and oxidation potentials (0.03 - 0.110 V) with respect to MTPP. This indicates that the presence of electron withdrawing substituent(s) at the  $\beta$ -pyrrole position(s) make the porphyrin ring easily reducible and difficult to oxidize relative to MTPP. Among all, MTPP(CHO)Br<sub>2</sub> exhibited more anodic shift than other  $\beta$ -substituted derivatives due to electron withdrawing CHO and Br substituents which enhance the electron deficient nature of  $\pi$ -system as compared to other mono-substituted porphyrins MTPP(X) (X = CHO, COOH) and MTPP as well. Cathodic shift has been observed for MTPP(CH<sub>2</sub>OH) relative to MTPPs and other derivatives (MTPP(X)Y<sub>2</sub>) which can be explained on the basis of electron donating nature of CH<sub>2</sub>OH group. The electron donating effect of -CH<sub>2</sub>OH group on porphyrin ring make it electron rich which facilitates facile oxidation and renders it ineffective for reduction. Both electron donating and electronwithdrawing substituents exhibited opposite effect on porphyrin ring which produce different redox behaviour. So, the presence of electron withdrawing groups (CHO, COOH, Br) cause an anodic shift in their redox potentials due to its inductive effect on porphyrin macrocycle while electron donating group (CH<sub>2</sub>OH) show cathodic shift in redox potential relative to unsubstituted porphyrin macrocycle. It can be observed that the electrochemical shift in the redox potential are more manifested due to pyrrole substitution as compared to the substitution at *meso*-phenyl ring of porphyrin systems.<sup>32</sup>

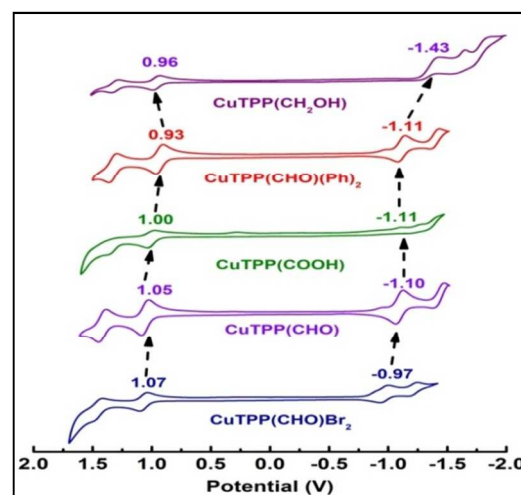


**Figure 4.** Cyclic voltammograms of CuTPP(X)Y<sub>2</sub> (X = CHO, COOH, and CH<sub>2</sub>OH; Y = H, Br, and Ph) in CH<sub>2</sub>Cl<sub>2</sub> containing 0.1 M TBAP with a scan rate of 0.1 V/s at 298 K.

The difference between the first ring oxidation and reduction potential tells about energy gap ( $\Delta E$ ) between the HOMO and LUMO of the porphyrin derivatives.<sup>33</sup>

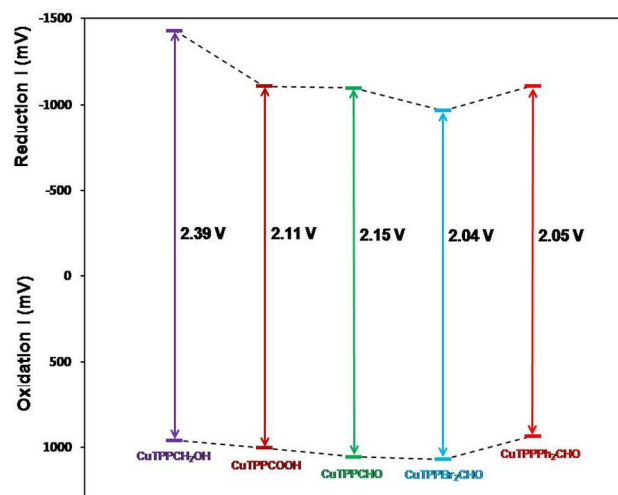


Figure 5. Effect of  $\beta$ -substituents and HOMO-LUMO variation of  $\text{CuTPP(X)Y}_2$ .

Table 2 indicates that  $\text{MTPP(X)Y}_2$  exhibited more anodic shift in first reduction potential as compared to first oxidation potential that of corresponding MTPPs. This seems to suggest that LUMO are more stabilized than HOMO. Fig. 5 represent the HOMO-LUMO gap variation of  $\text{CuTPP(X)Y}_2$  and Fig. S27 in the ESI represent for free base and other metal complexes. It is seen that **2** exhibited larger HOMO-LUMO gap than other derivatives and the trend is follow the order:  $\text{MTPP} \approx \text{MTPP}(\text{CH}_2\text{OH}) > \text{MTPP}(\text{COOH}) > \text{MTPP}(\text{CHO}) > \text{MTPP}(\text{CHO})\text{Br}_2 > \text{MTPP}(\text{CHO})\text{Ph}_2$ . It can be explained on the basis of electronic effect of the substituents where electronic withdrawing groups decrease the electron density on the porphyrin  $\pi$ -system, while electron donating hydroxymethyl group exhibit an opposite effect.

### Frontier and Subfrontier Orbitals Calculations

Gouterman's four orbital model designates  $a_{1u}$ ,  $a_{2u}$  are HOMOs while  $e_g$ s are LUMOs. *Meso*-substitution preferentially affects  $a_{2u}$ , whereas  $\beta$ -substitution largely influences  $a_{1u}$  as previously reported by Shelnutt *et al.*<sup>34</sup> Even though Binstead *et al* have reported the effect of  $\beta$ -substitution on  $\text{CuTPP}$  but their studies were limited to mono  $\beta$ -substitution.<sup>35</sup> Herein, we present the effect of mono- and tri-substitution on  $a_{1u}$  and  $a_{2u}$ . It is known that both  $a_{1u}$  and  $a_{2u}$  are nearly degenerate in which  $a_{2u}$  is slightly above than  $a_{1u}$  in  $\text{MTPP}$ .<sup>35</sup>

The electron withdrawing groups such as CHO, Br, COOH groups at  $\beta$ -position(s) stabilize  $a_{1u}$  to a greater extent than  $a_{2u}$  i.e.  $a_{1u} < a_{2u}$  (Figure 6). However, an opposite effect was observed for electron donating substituents such as Ph and  $\text{CH}_2\text{OH}$  i.e.  $a_{1u} > a_{2u}$ . In general, as the number of electron acceptor group increases on TPP skeleton, the stabilization of  $a_{1u}$  as well as  $e_g$  increases (Figure 6). For example, the difference between relative energies

of  $a_{1u}$  ( $\Delta a_{1u}$ ) of **4d** and **2d** is differ by 0.27 eV whereas the difference in energies of corresponding  $a_{2u}$  is 0.19 eV.

A concise illustration of frontier and subfrontier orbitals of  $\text{MTPP(X)Y}_2$  is listed in Tables 3 and S4-S6 in the ESI.

Table 3. The shift in energy levels of  $\text{NiTPP(X)Y}_2$  with respect to  $\text{NiTPP}$ , calculated using redox potentials and absorption spectral data

| Por                   | $E_{cg}$ (eV) | $I_{ox}$ | $I_{red}$ | $\Delta E^*(\text{eV})$ |                 |                  | $\delta e_j$ (eV) | $\delta e_i$ (eV) | $\delta e_k$ (eV) |
|-----------------------|---------------|----------|-----------|-------------------------|-----------------|------------------|-------------------|-------------------|-------------------|
|                       |               |          |           | $\Delta E_{cg}$         | $\Delta I_{ox}$ | $\Delta I_{red}$ |                   |                   |                   |
| NiTPP                 | 2.61          | 1.02     | -1.28     |                         |                 |                  |                   |                   |                   |
| <b>1d</b>             | 2.60          | 1.10     | -1.10     | -0.01                   | 0.08            | 0.18             | -0.08             | -0.25             | -0.18             |
| <b>2d<sup>a</sup></b> | 2.63          | 1.08     | -1.25     | 0.01                    | 0.06            | 0.03             | -0.06             | -0.03             | -0.03             |
| <b>3d</b>             | 2.67          | 1.01     | -1.40     | 0.06                    | -0.01           | -0.12            | 0.01              | 0.11              | 0.12              |
| <b>4d</b>             | 2.57          | 1.24     | -0.96     | -0.05                   | 0.22            | 0.32             | -0.22             | -0.33             | -0.32             |
| <b>5d</b>             | 2.56          | 1.07     | -1.10     | -0.06                   | 0.05            | 0.18             | -0.05             | -0.19             | -0.18             |

<sup>45</sup>  $E_{cg} = (E_B + E_Q)/2$ ;  $E_{B,Q} = 1240/\lambda_{B,Q}$ , a except  $\text{CH}_2\text{OH}$ , all values calculated with respect to  $\text{NiTPP}$  as electron removal from  $a_{2u}$ .

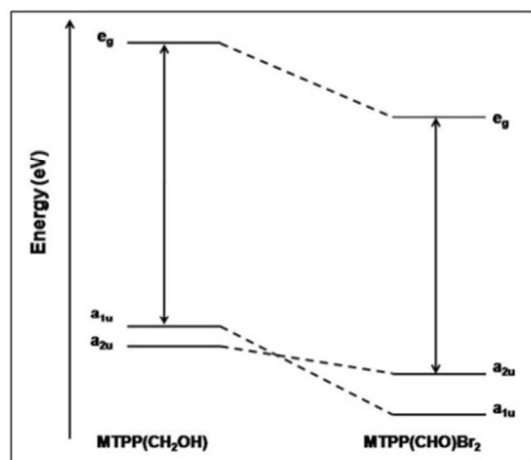


Figure 6. Effect of electron withdrawing  $\beta$ -substituents on frontier orbitals (HOMO and LUMO levels) of  $\text{MTPP}(\text{CH}_2\text{OH})$ .

### Conclusions

The present work demonstrates the synthesis, spectral and electrochemical redox properties of mono and tri- $\beta$ -substituted porphyrins,  $\text{H}_2\text{TPP(X)Y}_2$  ( $X = \text{CHO}, \text{COOH}, \text{CH}_2\text{OH}$ ;  $Y = \text{H}, \text{Br}, \text{Ph}$ ) and their metal (Co(II), Ni(II), Cu(II), and Zn(II)) complexes. We optimized the reaction condition for  $\text{H}_2\text{TPP}(\text{CHO})\text{Br}_2$  (**4**) which can be easily prepared in a good yield within 24 h. DFT optimised geometries revealed the fact that mono-substituted porphyrins (**1-3**) are exhibiting very slight distortion or nearly planar structure from the mean porphyrin plane but as steric crowding increases at  $\beta$ -pyrrole positions, tri-substituted porphyrins (**4** and **5**) show moderate non-planarity from the mean plane. All synthesized porphyrins exhibited red-shifted electronic spectra than MTPPs and  $\text{MTPP}(\text{CH}_2\text{OH})$  which is ascribed due to the electron withdrawing groups present at  $\beta$ -pyrrole position(s). The redox tunability was achieved by introducing electron donors ( $\text{CH}_2\text{OH}$  and Ph) and acceptor (CHO, COOH and Br) groups on



MTPP skeleton leading to dramatic cathodic and anodic shifts, respectively. Dramatic reduction in HOMO-LUMO gap with increase in  $\Delta a_{1u}$  was observed as the number of electron withdrawing groups increased. The mono- and tri- $\beta$ -substitution bring tunable optical absorption spectral features and electrochemical redox properties with modulated frontier orbitals which are interpreted in terms of both an inductive and resonance interactions of substituent(s) on porphyrin  $\pi$ -system. To the best of our knowledge, fluorescence spectral and tunable electrochemical redox properties of MTPP(X)Y<sub>2</sub> are not known in the literature.

## Acknowledgements

We are grateful for the support provided by Council of Scientific and Industrial Research (01(2694)/12/EMR-II), Science and Engineering Research Board (SB/FT/CS-015/2012) and Board of Research in Nuclear Science (2012/37C/61/BRNS/2776). We thank Dr. Jay Singh Meena, Post Doctoral Fellow, IISER Pune, for DFT Optimisation work. KP and RK thanks Ministry of Human Resource Development (MHRD), India for the senior research fellowship.

## Notes and references

Department of Chemistry, Indian Institute of Technology Roorkee, Roorkee-247667, Uttarakhand, India.

†Electronic Supplementary Information (ESI) available: Synthetic scheme and UV-Vis., fluorescence, <sup>1</sup>H NMR spectra of **1-5** and their metal complexes. CV figures and schematic variation HOMO-LUMO energy levels of MTPP(X)Y<sub>2</sub> are shown.

- (1) (a) B. M. Hoffman, *The Porphyrins*, Vol. 8, Ed.: D. Dolphin, *Academic Press, San Diego*, 1979, 403. (b) G. S. McDermott, M. Prince, A. A. Freer, A. M. Hawthornthwaite-Lawless, M. Z. Papiz, R. J. Cogdell and N. W. Isaacs, *Nature*, 1995, **374**, 517. (c) J. P. Glusker, *In Vitamin B<sub>12</sub>*, Ed.: D. Dolphin, *John Wiley and Sons, New York*, 1982, **1**, 23. (d) J. S. Summers, J. L. Petersen and A. M. Stolzenberg, *J. Am. Chem. Soc.*, 1994, **116**, 7189. (e) J. R. Lancaster, *The bioinorganic chemistry of Nickel*, *VCH Publishers, New York*, 1988, pp 141. (f) D. Qiu, M. Kumar, S. W. Ragsdale and T. G. Spiro, *Science*, 1994, **264**, 817. (g) *Cytochrome P-450: Structure, Mechanism, and Biochemistry*, Ed.: P. R. Ortiz de Montellano, *Plenum Press, New York*, 1986, 1. (h) M. W. Grinstead, M. G. Hill, J. A. Labinger and H. B. Gray, *Science*, 1994, **264**, 1311.
- (2) (a) G. Simonneaux and P. Le Maux, *Coord. Chem. Rev.*, 2002, **228**, 43. (b) D. Dolphin, T. G. Traylor and L.Y. Xie, *Acc. Chem. Res.*, 1997, **30**, 251 and references therein. (c) J. Y. Lee, O. K. Farha, J. Roberts, K. A. Scheidt, S. T. Nguyen and J. T. Hupp, *Chem. Soc. Rev.*, 2009, **38**, 1450. (d) S. Y. Ding and W. Wang, *Chem. Soc. Rev.*, 2013, **42**, 548. (e) W. Liu and J. T. Grooves, *Acc. Chem. Res.*, 2015, **48**, 1727. (f) W. Zhang, P. Jiang, Y. Wang, J. Zhang and P. Zhang, *Catal. Sci. Technol.*, 2015, **5**, 101.
- (3) (a) M. Ethirajan, Y. Chen, P. Joshi and R. K. Pandey, *Chem. Soc. Rev.*, 2011, **40**, 340. (b) I. J. Macdonald and T. J. Dougherty, *J. Porphyrins Phthalocyanines*, 2001, **5**, 105. (c) K. Lang, J. Mosinger and D. M. Wagnerova, *Coord. Chem. Rev.*, 2004, **248**, 321 and references therein. (d) R. K. Pandey, R. Zheng, in *The Porphyrin Handbook*, Vol. 6, Eds.: K. M. Kadish, K. M. Smith, R. Guilard, *Academic Press, New York*, 2000, pp 157.
- (4) (a) M. O. Senge, M. Fazekas, E. G. A. Notaras, W. J. Blau, M. Zawadzka, O. B. Locos and E. M. Ni. Mhuirheartaigh, *Adv. Mater.*, 2007, **19**, 2737 and references therein (b) M. Zawadzka, J. Wang, W. J. Blau and M. O. Senge, *Photochem. Photobiol. Sci.*, 2013, **12**, 996 and references therein.
- (5) (a) L. Li and E. W. G. Diau, *Chem. Soc. Rev.*, 2014, 291 and references therein. (b) F. Odobel, L. L. Pleux, Y. Pellegrin and E. Blart, *Acc. Chem. Res.*, 2010, **43**, 1063. (c) M. Urbani, M. Gratzel, Md. K. Nazeeruddin and T. Torres, *Chem. Rev.*, 2014, **114**, 12330 and references therein. (d) W. M. Campbell, A. K. Burrell, D. L. Officer and K. W. Jolly, *Coord. Chem. Rev.*, 2004, **248**, 1363. (e) C. P. Lee, R. Y. Lin, L.Y. Lin, C. T. Li., T. C. Chu, S. S. Sun, J. T. Lin and K. C. Ho, *RSC Adv.*, 2015, **5**, 23810 and references therein.
- (6) R. H. Jin, *Chem. Commun.*, 2002, 198.
- (7) (a) E. Galoppini, J. Rochford, H. Chen, G. Saraf, Y. Lu, A. Hagfeldt and G. Boschloo, *J. Phys. Chem. B*, 2006, **110**, 16159. (b) J. Rochford, D. Chu, A. Hagfeldt and E. Galoppini, *J. Am. Chem. Soc.*, 2007, **129**, 4655. (c) J. Rochford and E. Galoppini, *Langmuir*, 2008, **24**, 5366. (d) *The Porphyrin Handbook*, Vol. 8, Eds.: K. M. Kadish, K. M. Smith and R. Guilard, *Academic Press, New York*, 2000, pp 1. (e) *The Porphyrin Handbook*, Vol. 18, Eds.: K. M. Kadish, K. M. Smith and R. Guilard, *Academic Press, New York*, 2000, pp 1.
- (8) (a) J. A. Shelnut, X. Z. Song, J. G. Ma, S. L. Jia, W. Jentzen and C. J. Medforth, *Chem. Soc. Rev.*, 1998, **27**, 31 and reference therein. (b) Z. Shi, R. Franco, R. Haddad, J. A. Shelnut and G. C. Ferreira, *Biochemistry*, 2006, **45**, 2904. (c) B. Morgan and D. Dolphin, *Struct. Bonding*, 1987, **64**, 115. (d) M. Mumentau and C. A. Reed, *Chem. Rev.*, 1994, **94**, 659 and references therein.
- (9) (a) M. Gouterman, *In the Porphyrin*, Vol 3, Eds.: D. Dolphin, *Academic Press, New York*, 1978, pp 59. (b) R. H. Felton, *In the Porphyrin*, Vol 5, Eds.: D. Dolphin, *Academic Press, New York*, 1978, pp 127.
- (10) (a) M. O. Senge, *In The Porphyrin Handbook*, Vol. 1, Eds.: K. M. Kadish, K.M. Smith and R. Guilard, *Academic Press, New York*, 2000, pp. 239 and references therein. (b) M. O. Senge, *Chem. Commun.*, 2006, 243.
- (11) (a) J. E. Falk, *Porphyrins and Metalloporphyrins*, Elsevier, New York, N. Y., 1964, pp 28, 42, 69, 96. (b) M. Meot-Ner and A. D. Adler, *J. Am. Chem. Soc.*, 1975, **97**, 5107. (c) W. S. Caughey, W. Y. Fulimoto and B. P. Johnson, *Biochemistry*, 1966, **5**, 3830.
- (12) (a) B. D. McLees and W. S. Caughey, *Biochemistry*, 1968, **7**, 642; (b) W. S. Caughey, R. M. Deal, B. D. McLees and J. O. Alben, *J. Am. Chem. Soc.*, 1962, **84**, 1735. (c) M. Meot-Ner and A. D. Adler, *J. Am. Chem. Soc.*, 1972, **94**, 4763. (d) F.A. Walker, E. Hui and J. M. Walker, *J. Am. Chem. Soc.*, 1975, **97**, 2390.
- (13) J. H. Chou, M. E. Kosal, H. S. Nalwa, N. A. Rakow and K. S. Suslick, *In The Porphyrin Handbook*, Vol. 6, Eds.: K. M. Kadish, K. M. Smith and R. Guilard, *Academic Press, New York*, 2000, pp 44 and reference therein.
- (14) (a) A. W. Stephenson, P. Wagner, A. C. Partridge, K. W. Jolley, V. V. Filichev and D. L. Officer, *Tetrahedron Lett.*, 2008, **49**, 5632. (b) D. P. Arnold, R. Gaete-Holmes, A. W. Johnson, A. R. P. Smith and G. A. Williams, *J. Chem. Soc., Perkin. Trans. 1*, 1978, 1660. (c) D. P. Arnold, A. W. Johnson and M. Mahendran, *J. Chem. Soc., Perkin. Trans. 1*, 1978, 366. (d) L. Jaquinod, D. J. Nurco, C. J. Medforth, R. K. Pandey, T. P. Forsyth, M. M. Olmstead and K. M. Smith, *Angew. Chem. Int. Ed.*, 1996, **35**, 1013. (e) L. Witte and J. H. Fuhrhop, *Angew. Chem. Int. Ed.*, 1975, **14**, 361. (f) H. Tamiaki and M. Kouraba, *Tetrahedron*, 1997, **53**, 10677. (g) H. J. Callot, *Tetrahedron*, 1973, **29**, 899.
- (15) A. Giraudeau, H. J. Callot, J. Jordan, I. Ezhar and M. Gross, *J. Am. Chem. Soc.*, 1979, **101**, 3857.
- (16) A. Giraudeau, H. J. Callot and M. Gross, *Inorg. Chem.*, 1979, **18**, 201.
- (17) A. Giraudeau, A. Louati, H. J. Callot and M. Gross, *Inorg. Chem.*, 1981, **20**, 769.
- (18) R. A. Binstead, M. J. Crossley and N. S. Hush, *Inorg. Chem.*, 1991, **30**, 1259.
- (19) (a) Y. Terazono, B. O. Patrick and D. Dolphin, *Inorg. Chem.*, 2002, **41**, 6703. (b) Y. Terazono and D. Dolphin, *J. Org. Chem.*, 2003, **68**, 1892.
- (20) K. M. Kadish, G. Royal, E. V. Caemelbecke and L. Gueletti, *In The Porphyrin Handbook*, Vol. 9, Eds.: K. M. Kadish, K. M. Smith and R. Guilard, *Academic Press, New York*, 2000, pp 59 and references therein.
- (21) F. D'Souza, M. Zandler, P. Tagliatesta, Z. Ou, J. Shao, E. Van Caemelbecke and K. M. Kadish, *Inorg. Chem.*, 1998, **37**, 4567.

- (22) P. Ochsenbein, K. Ayougou, D. Mandon, J. Fischer, R. Weiss, R. N. Austin, K. Jayaraj, A. Gold, J. Terner and J. Fajer, *Angew. Chem. Int. Ed.*, 1994, **33**, 348.
- (23) (a) M. O. Senge, V. Gerstung, K. Ruhlandt-Senge, S. Runge and I. Lehmann, *J. Chem. Soc., Dalton Trans.*, 1998, 4187. (b) H. Duval, V. Bulach, J. Fischer and R. Weiss, *Inorg. Chem.*, 1999, **38**, 5495. (c) L. Jaquinod, R. G. Khoury, K. M. Shea and K. M. Smith, *Tetrahedron*, 1999, **5**, 13151. (d) J. Leroy, E. Porhiel and A. Bondon, *Tetrahedron*, 2002, **58**, 6713. (e) P. Bhyrappa, M. Sankar and B. Varghese, *Inorg. Chem.*, 2006, **45**, 4136. (f) P. Bhyrappa, C. Arunkumar and B. Varghese, *Inorg. Chem.*, 2009, **48**, 3954. (g) J. Chen, K. L. Li, Y. Guo, C. Liu, C. C. Guo and Q. Y. Chen, *RSC Adv.*, 2013, **3**, 8227. (h) Y. Fang, P. Bhyrappa, Z. Ou and K. M. Kadish, *Chem. Eur. J.*, 2014, **20**, 524.
- (24) E. E. Bonfantini, A. K. Burrell, W. M. Campbell, M. J. Crossley, J. J. Gosper, M. M. Harding, D. L. Officer and D. C. W. Reid, *J. Porphyrins Phthalocyanines*, 2002, **6**, 708.
- (25) (a) P. Bhyrappa, V. Velkannan and A. Maity, *J. Porphyrins Phthalocyanines*, 2010, **14**, 459. (b) L. Jaquinod, R. G. Khoury, K. M. Shea and K. M. Smith, *Tetrahedron*, 1999, **55**, 13151.
- (26) P.S. Reeta, J. Kandhadi and G. Lingamallu, *Tetrahedron Letters*, 2010, **51**, 2856.
- (27) (a) A. Ghosh, *Acc. Chem. Res.*, 1998, 31, 189. (b) A. Ghosh, In *The Porphyrin Handbook*, Eds.: K. M. Kadish, R. Guilard and K. M. Smith, *Academic Press, San Diego, CA*, 1999, **7**, 1. (c) A. Ghosh and E. Steene, *J. Biol. Inorg. Chem.*, 2001, **6**, 739. (d) A. Ghosh and P. R. Taylor, *Curr. Opin. Chem. Biol.*, 2003, 91, 113. (e) A. Ghosh, *J. Biol. Inorg. Chem.*, 2006, 11, 712. (f) K. E. Thomas, I. H. Wasbotten and A. Ghosh, *Inorg. Chem.*, 2008, 47, 10469. (g) A. B. Alemayehu, L. K. Hansen and A. Ghosh, *Inorg. Chem.*, 2010, 49, 7608.
- (28) (a) P. Bhyrappa and V. Velkannan, *J. Chem. Sci.*, 2015, 127, **4**, 663. (b) R. Kumar and M. Sankar, *Inorg. Chem.*, 2014, **53**, 12706.
- (29) J. A. Shelnutt, X. Z. Song, J. G. Ma, S. L. Jia, W. Jentzen and C. J. Medforth, *Chem. Soc. Rev.*, 1998, **27**, 31 and references therein.
- (30) M. J. Gouterman, *Chem. Phys.*, 1959, **30**, 1139.
- (31) T. Takeuchi, H. B. Gray and W. A. Goddard III, *J. Am. Chem. Soc.*, 1994, **116**, 9730.
- (32) K. M. Kadish, *Prog. Inorg. Chem.*, 1986, **34**, 435.
- (33) J. H. Fuhrhorp, K. M. Kadish and D. G. Davis, *J. Am. Chem. Soc.*, 1973, **95**, 5140.
- (34) J. A. Shelnutt and V. Ortiz, *J. Phys. Chem.*, 1985, **89**, 4733 and references therein.
- (35) R. A. Binstead, M. J. Crossely and N. S. Hush, *Inorg. Chem.*, 1991, **30**, 1259.